

Identification and Reactivity of *s-cis,s-cis*-Dihydroxycarbene, a New [CH₂O₂] Intermediate

Henrik Quanz,^{||} Bastian Bernhardt,^{||} Frederik R. Erb, Marcus A. Bartlett, Wesley D. Allen,* and Peter R. Schreiner*

Cite This: <https://dx.doi.org/10.1021/jacs.0c09317>

Read Online

ACCESS |

Metrics & More

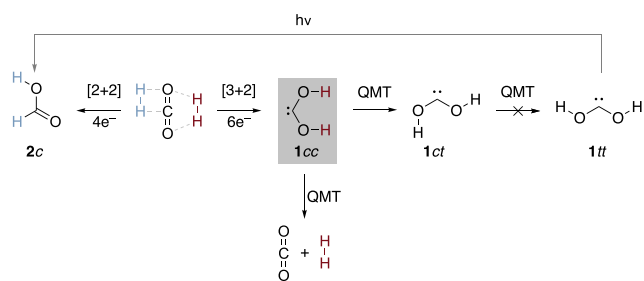
Article Recommendations

Supporting Information

ABSTRACT: We report the first preparation of the *s-cis,s-cis* conformer of dihydroxycarbene (**1cc**) by means of pyrolysis of oxalic acid, isolation of the lower-energy *s-trans,s-trans* (**1tt**) and *s-cis,s-trans* (**1ct**) product conformers at cryogenic temperatures in a N₂ matrix, and subsequent narrow-band near-infrared (NIR) laser excitation to give **1cc**. Carbene **1cc** converts quickly to **1ct** via quantum-mechanical tunneling with an effective half-life of 22 min at 3 K. The potential energy surface features around **1** were pinpointed by convergent focal point analysis targeting the AE-CCSDT(Q)/CBS level of electronic structure theory. Computations of the tunneling kinetics confirm the time scale of the **1cc** → **1ct** rotamerization and suggest that direct **1cc** → H₂ + CO₂ decomposition may also be a minor pathway. The intriguing latter possibility cannot be confirmed spectroscopically, but hints of it may be present in the measured kinetic profiles.

The fundamental chemistry of the [CH₂O₂] system is paramount to the grand challenges of energy storage and transportation as well as control of global warming. Moreover, as highly abundant molecules in space, H₂ and CO₂ may provide access to simple organic molecules in the atmosphere of prebiotic earth and extraterrestrial environments.^{1–3} Although the direct reduction of CO₂ with H₂ has a prodigious activation barrier (>80 kcal mol⁻¹), McCarthy et al.⁴ formed both *s-cis,s-trans*-dihydroxycarbene (**1ct**) (Scheme 1) and *s-*

Scheme 1. Formal Electrocyclic Reactions of H₂ + CO₂ Leading to *s-cis,s-cis*-Dihydroxycarbene (**1cc**), *s-cis*-Formic Acid (**2c**), and the Lower-Lying Rotamers of **1**



trans-formic acid (**2t**) by electric discharge of gaseous H₂ + CO₂ mixtures. This alternative route complements our original synthesis of **1ct** and *s-trans,s-trans*-dihydroxycarbene (**1tt**) based on pyrolysis of oxalic acid.⁵

The formation of **1** and subsequently **2** from H₂ + CO₂ potentially plays a role in the origin of life by trapping of H₂ from volcanic or other origins before its rapid escape into the atmosphere.⁶ As **2** is present in volcanic eruptions and black smokers,⁷ one viable route may involve **1** as a reactive intermediate. In a different vein, we have shown recently that

hydroxycarbenes react with carbonyl compounds to form sugars in the gas phase.⁸ Analogously, **1** may be a C₁ building block for amino acids through its reactions with imines.

In contrast to most hydroxycarbenes, at cryogenic temperatures **1** does not undergo a [1,2]-H shift via quantum-mechanical tunneling (QMT) to the associated carbonyl product **2** because strong oxygen lone-pair electron donation increases the accompanying barrier.⁴ Of the three possible dihydroxycarbene rotamers,¹⁰ **1tt** and **1ct** have been identified spectroscopically,^{4,5,11} but the higher-energy species *s-cis,s-cis*-dihydroxycarbene (**1cc**) has not been reported. Here we isolate and spectroscopically characterize **1cc**, document its conformational QMT to **1ct**, and explore the possibility of its direct dissociation into H₂ + CO₂ at very low temperatures.

The direct formation of **1** from H₂ and CO₂⁴ seems feasible only through the **1cc** rotamer, elevating the need to fully characterize this species. While **2c** is 44.6 kcal mol⁻¹ lower in energy than **1cc** (Figure 1), the activation barriers to form **1** and **2** from H₂ + CO₂ differ by less than 8 kcal mol⁻¹. Although the formation of **2** is formally a thermally forbidden^{12,13} four-electron [2 + 2] cycloaddition,^{14,15} it is kinetically favored in the absence of QMT over the allowed six-electron [3 + 2] reaction to give **1cc** (Scheme 1). However, the situation might change when QMT is taken into account, as this phenomenon leads to increased reaction rates, i.e., effectively lower activation barriers. The possible involvement of **1** in fundamental [CH₂O₂] chemistry has long been

Received: August 30, 2020

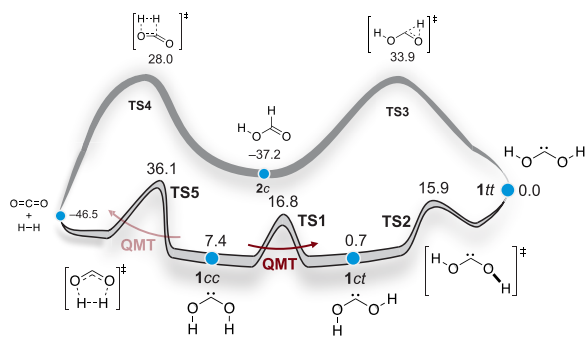
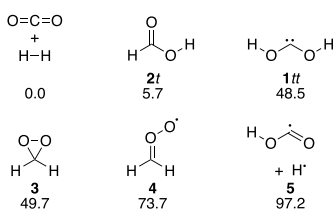


Figure 1. Pictorial presentation (not drawn to scale) of the converged FPA relative energies (ΔH_0 , in kcal mol^{-1}) of key species connected to **1**. Details of the computations are given in the SI.

Scheme 2. Relative Energies of the Experimentally Identified Species (Lowest-Energy Conformers) on the $[\text{CH}_2\text{O}_2]$ Potential Energy Surface (Computed FPA Relative Energies Are Given in kcal mol^{-1})



overlooked, as studies have mostly emphasized the Criegee intermediate **4**^{16,17} and dioxirane **3**,¹⁸ which are actually *higher* in energy (Scheme 2).

Here we follow our established route employing high-vacuum flash pyrolysis (HVFP) of oxalic acid (**6**) to first produce and trap **1tt** and **1ct** in a N_2 matrix at 3 K.⁵ To generate **1cc**, **1tt** and **1ct** were prepared first and then selectively irradiated with near-infrared (NIR) light from a narrow-band optical parametric oscillator (OPO) laser. Similar strategies have been used to detect higher-lying rotamers of other matrix-isolated compounds (e.g., formic acid).^{19–22} New electronic structure computations employing focal point analysis (FPA)^{23–27} were executed to obtain definitive energetics for the potential energy surface (PES) surrounding **1** (Figure 1) at the composite AE-CCSDT(Q)/CBS//AE-CCSD(T)^{28–32}/aug-cc-pCVTZ³³ level of theory.^{34,35} Tunneling half-lives were computed using both AE-CCSD(T)/aug-cc-pCVTZ reaction paths conjoined with the Wentzel–Kramers–Brillouin (WKB) method^{36–39} as well as density functional theory (DFT)^{40–46} curves treated with small-curvature tunneling (SCT) canonical variational theory (CVT).^{47,48}

In our optically transparent matrices resulting from deposition of the pyrolysis products on a cold window, selective vibrational excitation of **1tt** at $7026 \pm 4 \text{ cm}^{-1}$ gave **1ct** (Figures S2 and S3), while the back reaction was initiated with NIR irradiation at $6542 \pm 4 \text{ cm}^{-1}$ (Figure S3). After NIR irradiation at either of these two absorptions, we also observed new IR bands that vanished over the course of 1.5 h when the matrix was kept in the dark (Figure S4). We assigned these bands to the **1cc** conformer with the help of VPT2//AE-CCSD(T)/aug-cc-pCVTZ^{49,50} vibrational frequency computations (Figure 2); full details of the assignments, including total energy distributions,^{51–53} can be found in Table S3. The

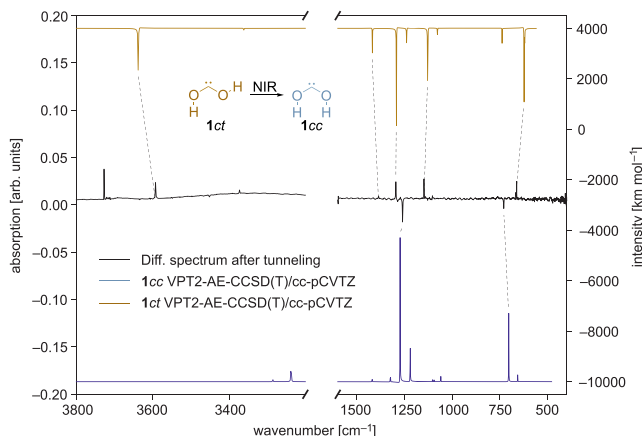


Figure 2. Dihydroxycarbene rotamers **1cc** and **1ct** identified in a N_2 matrix at 3 K. Bottom and top traces: computed VPT2//AE-CCSD(T)/aug-cc-pCVTZ spectra of **1cc** and **1ct**, respectively. Middle trace: difference spectrum obtained from spectra recorded before and after the matrix was irradiated at $7026.0 \pm 4 \text{ cm}^{-1}$ (**1tt** band) for 15 min and then at $6542 \pm 4 \text{ cm}^{-1}$ (**1ct** band) for 15 min and then kept in the dark for 1.5 h. The full spectrum is shown in Figure S4.^{54–56}

multireference character of **TS4** and **TS5** is marginal (cf. Chapter 4.3 in the Supporting Information (SI)).²⁵

While the bands of **1cc** vanished, the bands of **1ct** simultaneously grew. Because the barrier for this conformational interconversion is $9.4 \text{ kcal mol}^{-1}$ (Figure 1), QMT must be operative for this reaction to occur at 3 K. The disappearance of **1cc** over time (Figure 3) was monitored at

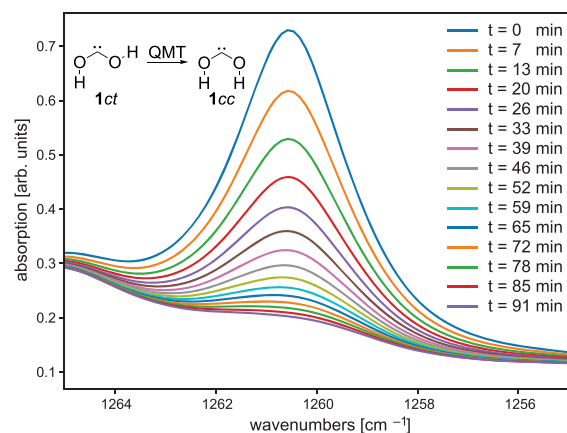


Figure 3. Temporal decay of the most intense IR band (1260.2 cm^{-1}) of **1cc** over 138 min at 3.0 K in a N_2 matrix. Spectra were taken every 98 s with a $4.5 \mu\text{m}$ low-pass filter in front of the matrix to avoid photoreactions caused by the spectrometer global source. For clarity, only every fourth trace is shown. The temporal profile of the **1cc** band at 730.1 cm^{-1} is shown in Figure S5.^{54–56}

different temperatures, and our kinetic analyses revealed effective tunneling half-lives in the 17–22 min range over the 3–20 K interval (Table 1). The relative insensitivity of the reaction rate to temperature is also indicative of QMT.

In solid Ar and Ne matrices, we could interconvert **1tt** and **1ct** by NIR irradiation, but the **1cc** rotamer remained undetected (Figures S7–S11). However, the bands of **1ct** could not be depleted completely even after prolonged irradiation, which might hint that **1cc** formed but has an inherent lifetime of less than 2 min in these environments. Our

Table 1. Tunneling Kinetics of *s-cis,s-cis*-Dihydroxycarbene (1cc) in a N₂ Matrix^a

T/K	τ_{ct}/h	τ_{leak}/h	τ_{eff}/h^b	leak fraction	initial 1cc:1ct population ratio
3.0	0.331(1)	0.78(10)	0.363	0.13(2)	2.797(3)
7.5	0.331(1)	0.73(9)	0.359	0.14(3)	2.106(3)
12.5	0.312(1)	0.48(12)	0.325	0.10(7)	3.483(3)
15.0	0.307(1)	0.82(22)	0.331	0.09(3)	4.255(5)
20.0	0.278(1)	0.35(7)	0.291	0.19(18)	3.133(3)

^aStandard errors of the least-squares fits are shown in parentheses in multiples of the last significant digit. See the text and SI for a description of the fitting parameters. ^b τ_{eff} = effective half-life for overall 1cc decay.

best theoretical prediction for the 1cc → 1ct tunneling half-life in the gas phase is 1.2 min, which was derived as follows: (a) uniform scaling of the optimized AE-CCSD(T)/aug-cc-pCVTZ potential energy curve (Table S30) by 1.024 to reproduce the converged FPA rotamerization barrier; (b) WKB evaluation of the tunneling half-life on this scaled curve; and (c) application of the SCT correction factor of 0.0363 given by the B3LYP/cc-pVTZ level of theory (Table S29). The resulting prediction is consistent with both the observed lack of 1cc bands in the Ar and Ne matrices and the measured 1cc half-life of 17–22 min in solid N₂, whose appreciable polarizability is known to stabilize reactive intermediates. Khriachtchev et al. reported a similar stabilization of the high-lying HOCO-conformer in N₂.¹⁹ To investigate this effect, we computed N₂ complexes of all three rotamers of 1 (SI Chapter 4.2), similar to those reported for formic acid.²⁰ The AE-CCSD(T)/aug-cc-pCVTZ-optimized complexes display O–H...N₂ interactions that yield binding energies of 1.2–1.8 kcal mol⁻¹ and vibrational frequency shifts as large as 63 cm⁻¹. Such substantial interactions are also evidenced in the experimental IR spectra of 1ct and 1tt, as both species display an O–H stretching frequency in N₂ that differs from the corresponding value in solid Ne (Tables S11 and S12) by almost 60 cm⁻¹.

The QMT kinetics from 3 to 20 K was analyzed by means of a simultaneous nonlinear least-squares fit of two 1cc and three 1ct high-quality IR bands (Table 1). The simplest integrated rate equations capable of accurately fitting the entirety of the kinetic data for 1cc decay and 1ct growth required four adjustable parameters: the rotamerization half-life (τ_{ct}), the 1cc:1ct initial population ratio, a half-life for alternative 1cc decay (τ_{leak}), and a branching fraction for such secondary leaking. Unlike the cases of carbonic⁵⁷ and oxalic acid,⁵⁸ no evidence of frozen molecules or distinct fast and slow conformational tunneling was found. Figures S19–S28 show that if the rate constants for 1cc decay and 1ct growth are set equal to one another, the spectral data cannot be fit precisely, revealing the necessity of the “leak” component. As shown in Table 1, leaking is responsible for roughly 10% of the decay, which is too small to allow the parameters for this unknown process to be pinned down to a high degree. Nonetheless, we believe that the kinetic profiles provide compelling evidence for a secondary, minor process of decay with a half-life less than but on the same order of magnitude as τ_{ct} .

One candidate for the leaking process is suggested by our CVT/SCT tunneling computations (Tables S29–S33) at several levels of theory, including CCSD(T)/aug-cc-pVTZ//B2-PLYP/aug-cc-pVTZ. To wit, the rate for the direct 1cc → H₂ + CO₂ decomposition is in the same time regime as the

rotamerization, in agreement with the kinetic analysis. Neither product can be monitored in our experiments because the CO₂ concentration after pyrolysis exceeds our spectrometer limits and H₂ is not IR-active. Continuously populating 1cc by laser irradiation of the other rotamers should lead to overall depletion of 1 to form H₂ and CO₂, but this was not observed after 5 h (Figure S6).

We attempted to probe the behavior of the dideuterated species ²H₂-1 originating from the pyrolysis of ²H₂-oxalic acid⁵ in order to further characterize 1cc and its tunneling decay (which should be quenched by dideuteration). However, bands of ²H₂-1cc were not observed after NIR excitation because the energy of the O–²H overtone of ²H₂-1tt is barely too low (5258 cm⁻¹ = 15.0 kcal mol⁻¹) to overcome the rotamerization barriers (1tt → 1ct = 15.9 and 1ct → 1cc = 16.1 kcal mol⁻¹).

We tried to prepare monodeuterated 1 through ester pyrolysis of several suitable precursors⁵⁹ (Scheme S1), hoping to use the OH group as an NIR antenna for remote rotamerization.⁶⁰ This would have allowed an indirect probe of the leak process because the heavier ²H-1cc isotopomer could not dissociate by QMT while rotamerization would still occur at approximately 50% of the rate of the parent molecule. However, in all of our attempts the carbene yield was too low through this alternative generation method (see the SI for details).

To conclude, we have isolated and characterized in solid N₂ the higher-lying *s-cis,s-cis* rotamer of dihydroxycarbene, which may be the missing link in the reduction of CO₂ with H₂ to form 1ct⁴ and subsequently formic acid. The 1cc species rapidly rotamerizes even at 3 K and could be identified only in stabilizing N₂ rather than noble gas cryogenic environments. A secondary QMT pathway involving dissociation of 1cc to H₂ + CO₂ is plausible according to theory and might be responsible for the biexponential characteristics measured in our decay profiles.

■ ASSOCIATED CONTENT

SI Supporting Information

The Supporting Information is available free of charge at <https://pubs.acs.org/doi/10.1021/jacs.0c09317>.

Full-matrix IR spectra after pyrolysis of 6 in N₂, Ar, and Ne; full matrix IR spectra after irradiation with NIR light in N₂, Ar, and Ne; full assignments of 1 in Ne and N₂; full PES around 1 at the FPA//AE-CCSD(T)/aug-cc-pCVTZ level of theory; geometries with all important bond lengths and angles; Cartesian coordinates of all molecules on the PES; detailed results of tunneling computations; details of the kinetic analysis; description of attempts to generate ²H₁-1 (PDF)

■ AUTHOR INFORMATION

Corresponding Authors

Peter R. Schreiner – Institute of Organic Chemistry, Justus Liebig University, D-35392 Giessen, Germany; orcid.org/0000-0002-3608-5515; Email: prs@uni-giessen.de

Wesley D. Allen – Center for Computational Quantum Chemistry and Department of Chemistry, University of Georgia, Athens, Georgia 30602, United States; Allen Heritage Foundation, Dickson, Tennessee 37055, United States; Email: wballen@uga.edu

Authors

Henrik Quanz – Institute of Organic Chemistry, Justus Liebig University, D-35392 Giessen, Germany

Bastian Bernhardt – Institute of Organic Chemistry, Justus Liebig University, D-35392 Giessen, Germany; orcid.org/0000-0002-7734-6427

Frederik R. Erb – Institute of Organic Chemistry, Justus Liebig University, D-35392 Giessen, Germany

Marcus A. Bartlett – Center for Computational Quantum Chemistry and Department of Chemistry, University of Georgia, Athens, Georgia 30602, United States

Complete contact information is available at:
<https://pubs.acs.org/10.1021/jacs.0c09317>

Author Contributions

^{||}H.Q. and B.B. contributed equally.

Notes

The authors declare no competing financial interest.

ACKNOWLEDGMENTS

We thank Dennis Gerbig for maintaining our computer clusters and André K. Eckhardt and Hans P. Reisenauer for fruitful discussions. B.B. thanks the Bayer Fellowship Program and the Deutscher Akademischer Austauschdienst for financial support during a research visit at the University of Georgia and the Fonds der Chemischen Industrie for a doctoral scholarship. This work was supported by the Volkswagen Foundation (“What is Life” Grant 92 748 to P.R.S.).

REFERENCES

- (1) Tian, F.; Toon, O. B.; Pavlov, A. A.; De Sterck, H. A Hydrogen-Rich Early Earth Atmosphere. *Science* **2005**, *308*, 1014–1017.
- (2) Kasting, J. F. Earth’s early atmosphere. *Science* **1993**, *259*, 920–926.
- (3) Herbst, E. The chemistry of interstellar space. *Chem. Soc. Rev.* **2001**, *30*, 168–176.
- (4) Womack, C. C.; Crabtree, K. N.; McCaslin, L.; Martinez, O.; Field, R. W.; Stanton, J. F.; McCarthy, M. C. Gas-Phase Structure Determination of Dihydroxycarbene, One of the Smallest Stable Singlet Carbenes. *Angew. Chem. Int. Ed.* **2014**, *53*, 4089–4092.
- (5) Schreiner, P. R.; Reisenauer, H. P. Spectroscopic Identification of Dihydroxycarbene. *Angew. Chem. Int. Ed.* **2008**, *47*, 7071–7074.
- (6) Jeans, J. *The Dynamical Theory of Gases*; Cambridge University Press: London, 1916; Vol. 1, p 436.
- (7) Allen, A. G.; Baxter, P. J.; Ottley, C. J. Gas and particle emissions from Soufrière Hills Volcano, Montserrat, West Indies: characterization and health hazard assessment. *Bull. Volcanol.* **2000**, *62*, 8–19.
- (8) Eckhardt, A. K.; Linden, M. M.; Wende, R. C.; Bernhardt, B.; Schreiner, P. R. Gas-phase sugar formation using hydroxymethylene as the reactive formaldehyde isomer. *Nat. Chem.* **2018**, *10*, 1141–1147.
- (9) Schreiner, P. R. Tunneling Control of Chemical Reactions: The Third Reactivity Paradigm. *J. Am. Chem. Soc.* **2017**, *139*, 15276–15283.
- (10) Feller, D.; Borden, W. T.; Davidson, E. R. A theoretical study of paths for decomposition and rearrangement of dihydroxycarbene. *J. Comput. Chem.* **1980**, *1*, 158–166.
- (11) Broderick, B. M.; McCaslin, L.; Moradi, C. P.; Stanton, J. F.; Doublerly, G. E. Reactive intermediates in ⁴He nanodroplets: Infrared laser Stark spectroscopy of dihydroxycarbene. *J. Chem. Phys.* **2015**, *142*, 144309–144316.
- (12) Hutschka, F.; Dedieu, A.; Leitner, W. Metathesis as a Critical Step for the Transition Metal Catalyzed Formation of Formic Acid from CO₂ and H₂? An Ab Initio Investigation. *Angew. Chem. Int. Ed. Engl.* **1995**, *34*, 1742–1745.

(13) Steigerwald, M. L.; Goddard, W. A., III The 2_s + 2_s Reactions at Transition Metals. 1. The Reactions of D₂ with Cl₂TiH⁺, Cl₂TiH, and Cl₂Sch. *J. Am. Chem. Soc.* **1984**, *106*, 308–311.

(14) Woodward, R. B.; Hoffmann, R. The Conservation of Orbital Symmetry. *Angew. Chem. Int. Ed. Engl.* **1969**, *8*, 781–853.

(15) Woodward, R. B.; Hoffmann, R. Stereochemistry of Electrocyclic Reactions. *J. Am. Chem. Soc.* **1965**, *87*, 395–397.

(16) Taatjes, C. A.; Meloni, G.; Selby, T. M.; Trevitt, A. J.; Osborn, D. L.; Percival, C. J.; Shallcross, D. E. Direct Observation of the Gas-Phase Criegee Intermediate (CH₂OO). *J. Am. Chem. Soc.* **2008**, *130*, 11883–11885.

(17) Wadt, W. R.; Goddard, W. A., III Electronic structure of the Criegee intermediate. Ramifications for the mechanism of ozonolysis. *J. Am. Chem. Soc.* **1975**, *97*, 3004–3021.

(18) Lovas, F. J.; Suenram, R. D. Identification of dioxirane (H₂COO) in ozone-olefin reactions via microwave spectroscopy. *Chem. Phys. Lett.* **1977**, *51*, 453–456.

(19) Lopes, S.; Domanskaya, A. V.; Fausto, R.; Räsänen, M.; Khriachtchev, L. Formic and acetic acids in a nitrogen matrix: Enhanced stability of the higher-energy conformer. *J. Chem. Phys.* **2010**, *133*, 144507–144514.

(20) Marushkevich, K.; Khriachtchev, L.; Lundell, J.; Domanskaya, A.; Räsänen, M. Matrix Isolation and Ab Initio Study of *Trans-Trans* and *Trans-Cis* Dimers of Formic Acid. *J. Phys. Chem. A* **2010**, *114*, 3495–3502.

(21) Pettersson, M.; Lundell, J.; Khriachtchev, L.; Räsänen, M. IR Spectrum of the Other Rotamer of Formic Acid, *cis*-HCOOH. *J. Am. Chem. Soc.* **1997**, *119*, 11715–11716.

(22) Gerbig, D.; Schreiner, P. R. Hydrogen-Tunneling in Biologically Relevant Small Molecules: The Rotamerizations of α -Ketocarboxylic Acids. *J. Phys. Chem. B* **2015**, *119*, 693–703.

(23) East, A. L. L.; Allen, W. D. The heat of formation of NCO. *J. Chem. Phys.* **1993**, *99*, 4638–4650.

(24) Schuurman, M. S.; Muir, S. R.; Allen, W. D.; Schaefer, H. F., III Toward subchemical accuracy in computational thermochemistry: Focal point analysis of the heat of formation of NCO and [H₂N,C,O] isomers. *J. Chem. Phys.* **2004**, *120*, 11586–11599.

(25) Bartlett, M. A.; Liang, T.; Pu, L.; Schaefer, H. F., III; Allen, W. D. The multichannel *n*-propyl + O₂ reaction surface: Definitive theory on a model hydrocarbon oxidation mechanism. *J. Chem. Phys.* **2018**, *148*, 094303.

(26) Császár, A. G.; Allen, W. D.; Schaefer, H. F., III In pursuit of the ab initio limit for conformational energy prototypes. *J. Chem. Phys.* **1998**, *108*, 9751–9764.

(27) Gonzales, J. M.; Allen, W. D.; Schaefer, H. F., III Model Identity S_N2 Reactions CH₃X + X⁻ (X = F, Cl, CN, OH, SH, NH₂, PH₂): Marcus Theory Analyzed. *J. Phys. Chem. A* **2005**, *109*, 10613–10628.

(28) Stanton, J. F. Why CCSD(T) works: a different perspective. *Chem. Phys. Lett.* **1997**, *281*, 130–134.

(29) Čížek, J. On the Correlation Problem in Atomic and Molecular Systems. Calculation of Wavefunction Components in Ursell-Type Expansion Using Quantum-Field Theoretical Methods. *J. Chem. Phys.* **1966**, *45*, 4256–4266.

(30) Bartlett, R. J.; Watts, J. D.; Kucharski, S. A.; Noga, J. Non-iterative fifth-order triple and quadruple excitation energy corrections in correlated methods. *Chem. Phys. Lett.* **1990**, *165*, 513–522.

(31) Purvis, G. D., III; Bartlett, R. J. A full coupled-cluster singles and doubles model: The inclusion of disconnected triples. *J. Chem. Phys.* **1982**, *76*, 1910–1918.

(32) Raghavachari, K.; Trucks, G. W.; Pople, J. A.; Head-Gordon, M. A fifth-order perturbation comparison of electron correlation theories. *Chem. Phys. Lett.* **1989**, *157*, 479–483.

(33) Woon, D. E.; Dunning, T. H., Jr. Gaussian basis sets for use in correlated molecular calculations. V. Core-valence basis sets for boron through neon. *J. Chem. Phys.* **1995**, *103*, 4572–4585.

(34) Kállay, M.; Nagy, P. R.; Mester, D.; Rolik, Z.; Samu, G.; Csontos, J.; Csóka, J.; Szabó, P. B.; Gyevi-Nagy, L.; Hégyel, B.; Ladjanszki, I.; Szegedy, L.; Ladóczki, B.; Petrov, K.; Farkas, M.; Mezei,

P. D.; Ganyecz, Á. MRCC, a Quantum-Chemical Program Suite. Available at <https://www.mrcc.hu>.

(35) MOLPRO, a Package of Ab Initio Programs, ver. 2019.2 (see the SI for the full reference). Available at <https://www.molpro.net>.

(36) Wentzel, G. Eine Verallgemeinerung der Quantenbedingungen für die Zwecke der Wellenmechanik. *Eur. Phys. J. A* **1926**, *38*, 518–529.

(37) Kramers, H. A. Wellenmechanik und halbzahlige Quantisierung. *Eur. Phys. J. A* **1926**, *39*, 828–840.

(38) Brillouin, L. La mécanique ondulatoire de Schrödinger: une méthode générale de résolution par approximations successives. *C. R. Acad. Sci.* **1926**, *183*, 24–26.

(39) Quanz, H.; Schreiner, P. R. TUNNEX: An easy-to-use Wentzel-Kramers-Brillouin (WKB) implementation to compute tunneling half-lives. *J. Comput. Chem.* **2019**, *40*, 543–547.

(40) Lee, C.; Yang, W.; Parr, R. G. Development of the Colle-Salvetti correlation-energy formula into a functional of the electron density. *Phys. Rev. B* **1988**, *37*, 785–789.

(41) Becke, A. D. A new mixing of Hartree–Fock and local density-functional theories. *J. Chem. Phys.* **1993**, *98*, 1372–1377.

(42) Becke, A. D. Density-functional exchange-energy approximation with correct asymptotic behavior. *Phys. Rev. A* **1988**, *38*, 3098–3100.

(43) Kim, K.; Jordan, K. D. Comparison of Density Functional and MP2 Calculations on the Water Monomer and Dimer. *J. Phys. Chem.* **1994**, *98*, 10089–10094.

(44) Stephens, P. J.; Devlin, F. J.; Chabalowski, C. F.; Frisch, M. J. Ab Initio Calculation of Vibrational Absorption and Circular Dichroism Spectra Using Density Functional Force Fields. *J. Phys. Chem.* **1994**, *98*, 11623–11627.

(45) Grimme, S. Semiempirical hybrid density functional with perturbative second-order correlation. *J. Chem. Phys.* **2006**, *124*, 034108.

(46) Bousquet, D.; Brémond, E.; Sancho-García, J. C.; Ciofini, I.; Adamo, C. Is There Still Room for Parameter Free Double Hybrids? Performances of PBE0-DH and B2PLYP over Extended Benchmark Sets. *J. Chem. Theory Comput.* **2013**, *9*, 3444–3452.

(47) Fernandez-Ramos, A.; Ellingson, B. A.; Garrett, B. C.; Truhlar, D. G. Variational transition state theory with multidimensional tunneling. *Rev. Comput. Chem.* **2007**, *23*, 125–233.

(48) Frisch, M. J.; et al. *Gaussian 16*, rev. B.01; Gaussian, Inc.: Wallingford, CT, 2016 (see the SI for the full reference). Available at <https://www.gaussian.com>.

(49) Allen, W. D.; Császár, A. G. On the ab initio determination of higher-order force constants at nonstationary reference geometries. *J. Chem. Phys.* **1993**, *98*, 2983–3015.

(50) Allen, W. D.; Császár, A. G.; Szalay, V.; Mills, I. M. General derivative relations for anharmonic force fields. *Mol. Phys.* **1996**, *89*, 1213–1221.

(51) Pulay, P.; Török, F. *Acta Chim. Acad. Sci. Hungary* **1965**, *44*, 287.

(52) Keresztury, G.; Jalsovszky, G. An alternative calculation of the vibrational potential energy distribution. *J. Mol. Struct.* **1971**, *10*, 304–305.

(53) Allen, W. D.; Császár, A. G.; Horner, D. A. The Puckering Inversion Barrier and Vibrational Spectrum of Cyclopentene. A Scaled Quantum Mechanical Force Field Algorithm. *J. Am. Chem. Soc.* **1992**, *114*, 6834–6849.

(54) Hunter, J.; Matplotlib, D. A 2D Graphics Environment. *Comput. Sci. Eng.* **2007**, *9*, 90–95.

(55) Behnel, S.; Bradshaw, R.; Citro, C.; Dalcin, L.; Seljebotn, D. S.; Smith, K. Cython: The Best of Both Worlds. *Comput. Sci. Eng.* **2011**, *13*, 31–39.

(56) van der Walt, S.; Colbert, S. C.; Varoquaux, G. The NumPy Array: A Structure for Efficient Numerical Computation. *Comput. Sci. Eng.* **2011**, *13*, 22–30.

(57) Wagner, J. P.; Reisenauer, H. P.; Hirvonen, V.; Wu, C.-H.; Tyberg, J. L.; Allen, W. D.; Schreiner, P. R. Tunneling in carbonic acid. *Chem. Commun.* **2016**, *52*, 7858–7861.

(58) Schreiner, P. R.; Wagner, J. P.; Reisenauer, H. P.; Gerbig, D.; Ley, D.; Sarka, J.; Császár, A. G.; Vaughn, A.; Allen, W. D. Domino Tunneling. *J. Am. Chem. Soc.* **2015**, *137*, 7828–7834.

(59) Honda, K.; Ohkura, S.; Hayashi, Y.; Kawauchi, S.; Mikami, K. Cationic Chiral Pd-Catalyzed “Acetylenic” Diels–Alder Reaction: Computational Analysis of Reversal in Enantioselectivity. *Chem. Asian J.* **2018**, *13*, 2842–2846.

(60) Halasa, A.; Reva, I.; Lapinski, L.; Nowak, M. J.; Fausto, R. Conformational Changes in Thiazole-2-carboxylic Acid Selectively Induced by Excitation with Narrowband Near-IR and UV Light. *J. Phys. Chem. A* **2016**, *120*, 2078–2088.